Electronic Supplementary Information

A GO-assisted method for the preparation of ultrathin covalent organic framework membranes for gas separation

*Yunpan Ying, Dahuan Liu**, *Jing Ma, Minman Tong, Weixin Zhang, Hongliang Huang, Qingyuan Yang and Chongli Zhong**

State Key Laboratory of Organic-Inorganic Composites and Beijing Advanced Innovation Center for Soft Matter Science and Engineering,

Beijing University of Chemical Technology, Beijing 100029, China

E-mail: liudh@mail.buct.edu.cn; zhongcl@mail.buct.edu.cn

Contents

1. Materials

$ZnCl_2$ (98 %) and 1, 4-dicyanobenzene (DCB, 98 %) were purchased from J&K. Single-layered GO powder prepared by modified Hummer's method was purchased from Nanjing JCNANO Tech Co., Ltd, China. Isopore cellulous acetate supports (with average pore size of about 100 nm) were purchased from Millipore. Ampoules (10 ml) were purchased from Synthware Glass Instrument Co., Ltd. H_2, CO_2 with purity > 99.999 % were purchased from Beiyang Special Gases Co., Ltd. Before usage, $ZnCl_2$ was dried in vacuum at 423 K overnight and DCB was purified by sublimation.

2. Preparation of GO nanosheets dispersion liquid

GO nanosheets dispersion liquid was obtained by ultra-sonication of GO powder in water and the supernatant was taken out after being centrifuged for 0.5 h at 10000 rpm.

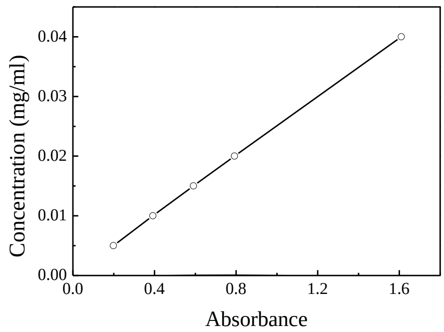

Fig. S1 The linear fit relationship between UV absorbance of the standard GO dispersions and their concentrations.

The concentration of the as-prepared GO dispersion was measured by UV-vis (TU-1901, Beijing general instrument Co., Ltd) with a pre-calibrated curve of GO concentration vs. absorption at about 225 nm wavelength, as shown in Fig. S1. From the linear fit diagram, we can obtain GO nanosheets dispersion with concentration of about 0.02 mg/ml.

3. Membranes Preparation

In a typical membrane preparation process, 25 ml of CTF-1 nanosheets dispersion liquid and 0.5 ml of GO nanosheets dispersion liquid were mixed ultrasonically for 1 h. The CTF-1 membrane was obtained by layer-by-layer restacking of the mixed nanosheets dispersion liquid onto isopore cellulous acetate support by a vacuum filtration system. Then the membranes were dried at room temperature for one day and further dried under vacuum at 313 K for 24 h, which were used for the following characterizations and gas permeation test. Membranes containing different amount of CTF-1 and GO nanosheets were prepared by the same method by controlling the amount of dispersion liquids. A schematic of the fabrication steps is shown in Fig. 1b.

4. Characterization Results

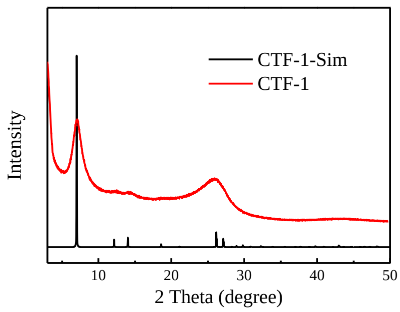

Fig. S2 PXRD pattern of prepared CTF-1 and the comparison with the simulated pattern.

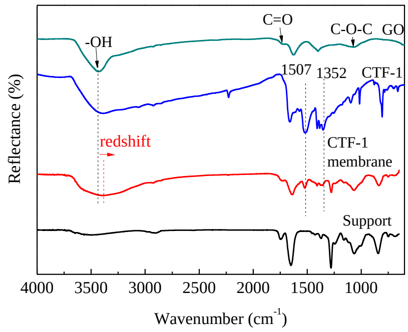

Fig. S3 FTIR of CTF-1 nanosheets membrane, CTF-1 powder, GO and bare support.

The absorption bands at 1352 cm^{-1} and 1507 cm^{-1} in FTIR (Fig. S3) points to the presence of triazine rings, indicating that the chemical structure of CTF-1 nanosheets remains unchanged during the restacking process. The -OH peak at around 3400 cm^{-1} in membranes has a slight shift (40 cm^{-1}) compared to that in GO nanosheets, demonstrating the change of –OH groups due to the interaction between GO and support.[2,3]

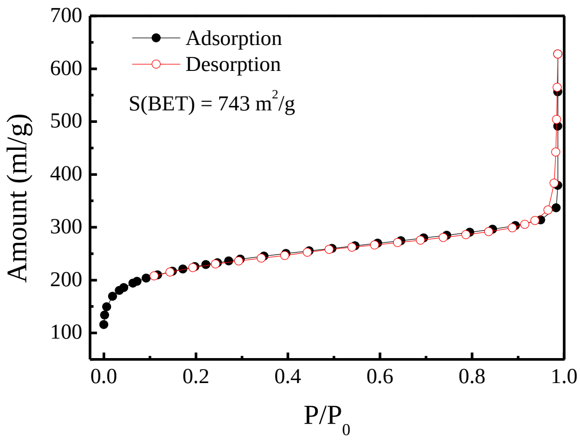

Fig. S4 N_2 adsorption-desorption isotherm at 77 K and BET surface area of CTF-1 powder.

Table S1. Elemental analyses of CTF-1 powder

Name	C (wt %)	N (wt %)	H (wt %)
CTF-1 as reported[1]	72.8	19.30	3.19
CTF-1 as calculated	75.0	21.86	3.15
CTF-1 in this work	73.2	18.88	3.28

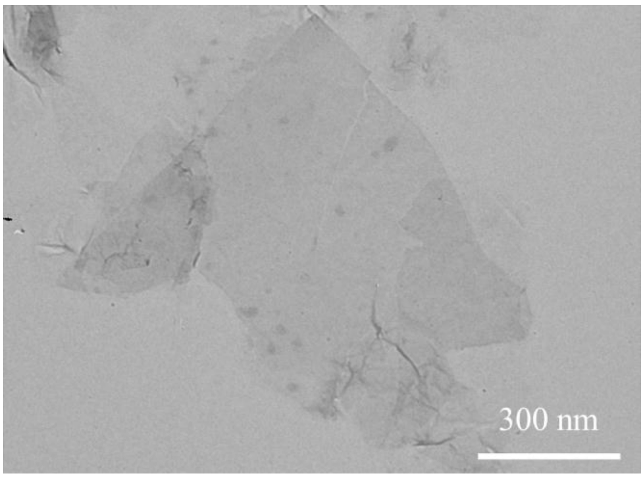

Fig. S5 TEM of GO nanosheets.

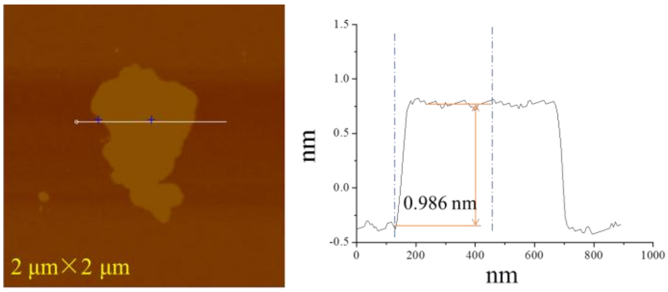

Fig. S6 AFM image and the corresponding height line of GO nanosheets.

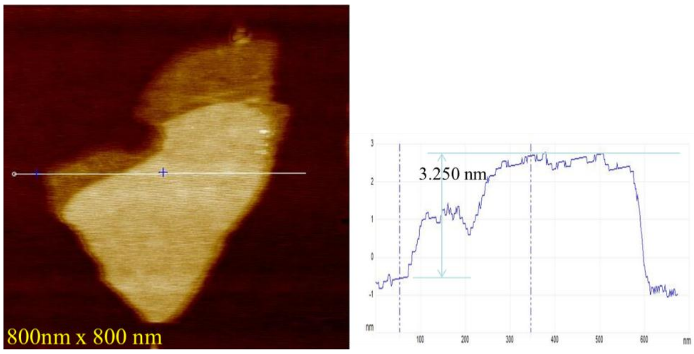

Fig. S7 AFM of the mixed CTF-1 and GO nanosheets.

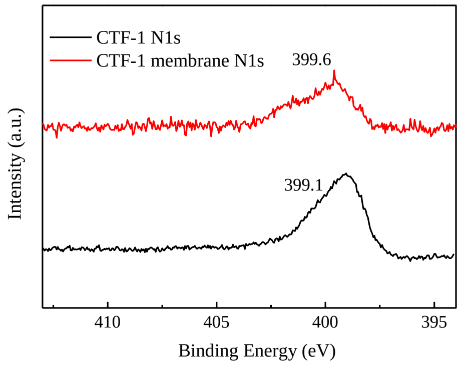

Fig. S8 XPS N1s spectra of the prepared 100-nm-thick CTF-1 membrane and CTF-1 powder.

Table S2. XPS data of CTF-1 powder and CTF-1 membrane

Elements	CTF-1 (eV)	CTF-1 membrane (eV)
N1s	399.1	399.6

XPS characterization for CTF-1 powder and CTF-1 membrane can indicate the interaction between GO and the N atoms of CTF-1. The N1s component peaks shift from 399.1(C=N, C-N) to 399.6 eV. This result showed a decreased electron cloud density of N atoms, suggesting that the N atoms of CTF-1 could form hydrogen bonds with the H atoms of GO. [4,5]

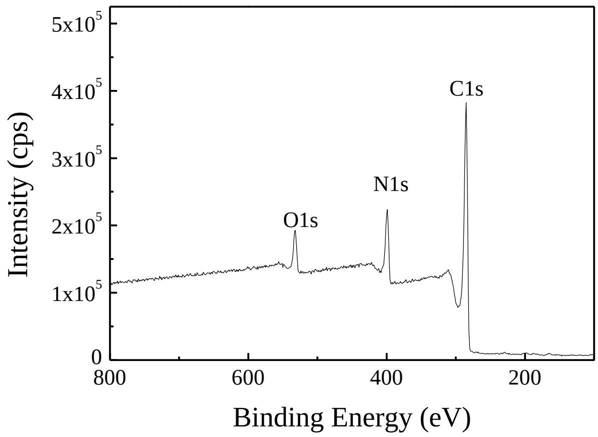

Fig. S9 XPS spectra of the prepared 100-nm-thick CTF-1 nanosheets membrane.

According to the XPS analysis in Fig. S6 and Table S3, we can find that C/N ratio in the membrane surface (5.86) is higher than that (3.89) in the CTF-1 powder according the elements analysis as displayed in Table S1. This indicates the presence of GO nanosheets on the membrane surface.

Table S3. Elements weight percent analysis result from the XPS spectra.

Elements	C	N	O
Weight percent (%)	80.69	13.78	5.53

5. Effect of GO amount on the separation performance

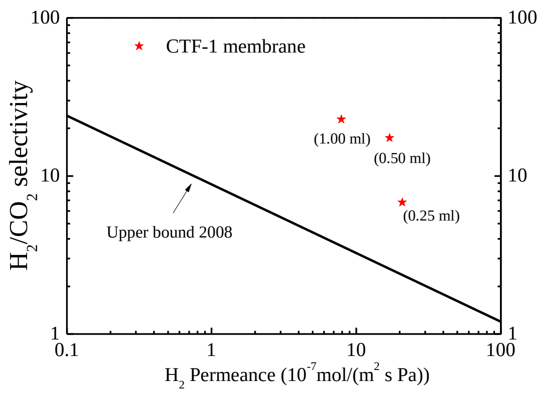

Fig. S10 Gas separation performance of CTF-1 membrane prepared by 25 ml of CTF-1 dispersion liquid and different amounts of GO dispersion liquid.

In order to determine the effect of the amount of GO in the membrane on the separation performance, we added different amounts of GO dispersion liquid (0.25 ml, 1.00 ml) into 25 ml of CTF-1 nanosheets dispersion liquid. Gas permeation experimental results (Fig. S8) show that when we use 0.25 ml of GO dispersion liquid the separation selectivity was very low and permeance was high. It can be concluded that this membrane has too many defects or voids which may induce the leak of gases. The balanced separation performances (both permeance and selectivity) become better with the increase of the GO dispersion liquid amount. While the H_2 permeance decreases to 7.9×10^{-7} mol/ (m^2s Pa) though with a slightly improvement in selectivity due to the impenetrability feature and the possible stacking of GO nanosheets. The farther parallel distance away from the upper bound (2008),[6] the better gas separation performance. Taking these in mind, we determined that the volume ratio of CTF-1 nanosheets dispersion liquid and GO nanosheets dispersion liquid was 50:1.

6. Effect of temperature on the separation performance

In order to study the effect of temperature on the separation performance, we conducted the gas permeation test at different temperatures (298 K, 313 K and 323 K) by taking the 100-

nm membrane as an example. From the results as shown in Fig. S11, it can be seen that when the permeation temperature was increased from 298 K to 323 K at 3 bars, the H_2 permeance increases from 1.7×10^{-6} mol/m^{2}s Pa to 2.8×10^{-6} mol/m^{2}s Pa, while the H_2/CO_2 selectivity decreases from 17.4 to 12.4. This phenomenon may be attributed to the interplay of adsorption and diffusion of H_2 and CO_2 in the CTF-1 membrane. The dependence of gas permeance on temperature is mainly depended on the relative values of activation energy for diffusion and exothermic heat of adsorption. Thus, the possible reason for the decrease of selectivity is the differences in the relative values of these two properties for H_2 and CO_2 with the increase of temperature. Similar tendency of temperature has been also found in other membranes[7-11].

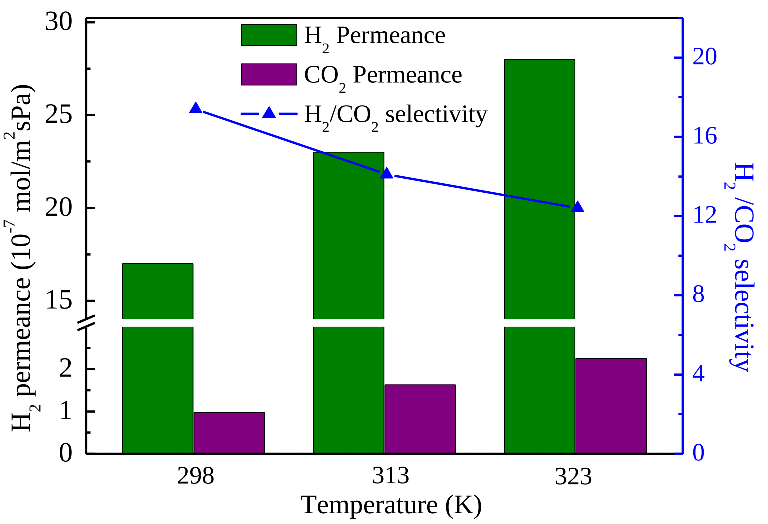

Fig. S11 Gas permeance (left-axis) and H_2/CO_2 selectivity (right-axis) as a function of temperature.

7. Thermal stability and durability

Thermal gravimetric analysis (TGA) of both the CTF-1 ultrathin membrane and bare support were conducted to study the thermal stability, as shown in Fig. S12. The obvious weight loss occurs at 430 K with 80 % of weight loss in the range of 430 K to 600 K, mainly attributing to the collapse of cellulous acetate support. Another stage of weight loss (about 12 %) is observed in the range of 600 K to 1200 K due to the collapse of CTF-1.

In order to check the durability of the membranes, we performed the gas permeation test of the 100-nm membrane up to 120 hours at 298 K and 323 K. As shown in Fig. S13, after a few hours for stabilization, the permeace and the H_2/CO_2 selectivity remain almost unchanged during the following test period, indicating the stability of these data.

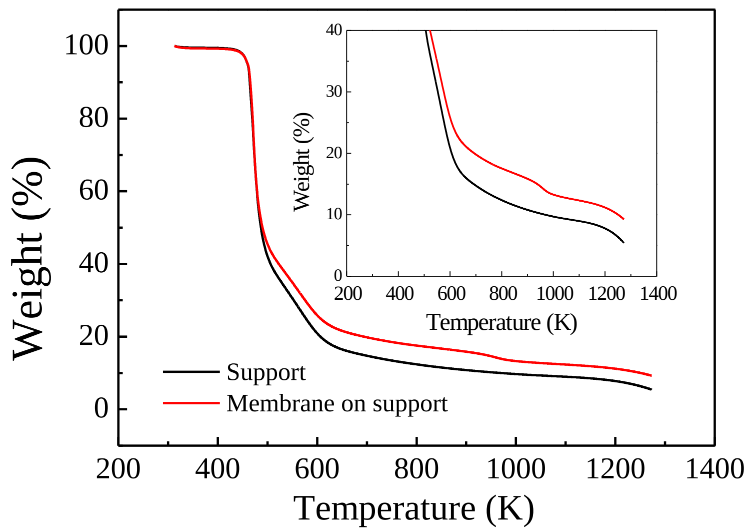

Fig. S12 TGA curves of the membrane and support.

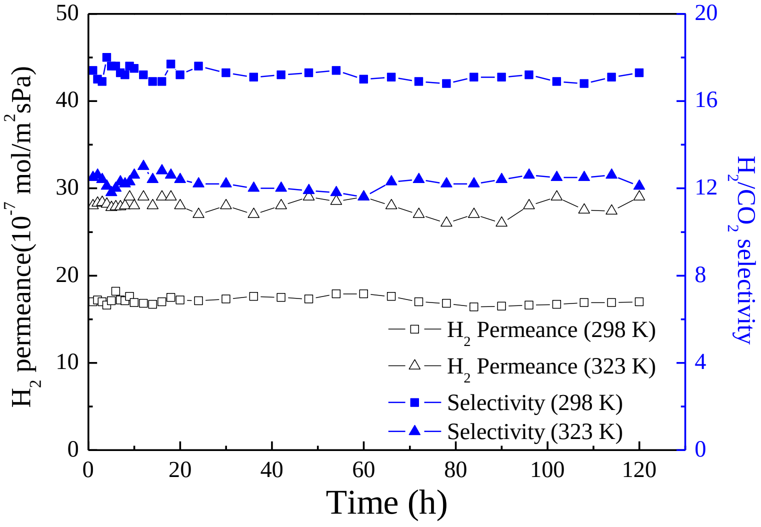

Fig. S13 Evolution of the gas permeance (left-axis) and H_2/CO_2 selectivity (right-axis) of the membrane.

8. Comparison with other membranes

Table S4. H_2/CO_2 separation performance in comparison to other membranes in literature.

Membranes	Thickness (nm)	Permeance (10^{-7} mol/(m^2s Pa))	Permeability (Barrers)	Selectivity	Reference
ZIF-8	6000	2.02	-	5.8	12
ZIF-7	1500	0.8	-	6.7	13
NH_2-MIL-53(Al)	15000	19.85	-	30.9	14
CAU-1	4000	1.08	-	12.34	15
HKUST-1	60000	10.6	-	6.84	16
ZIF-8@GO	-	1.27	-	14.9	17
ZIF-8/GO	100	0.546	-	1.6	18
CNT@IL/ZIF-9	30000	5.45	-	40.04	19
$Zn_2(bim)_4$ nanosheet membrane	-	9.16	-	291	20
MoS_2	17 35 60	91.9 23.6 8.19	-	3.4 3.7 4.4	21
Zeolite composite	5000	0.78	-	23	22

membrane					
ZIF-8/6FDA-Durene	10000	0.095	283.5	12	23
ZIF-7-PBI	-	-	26.2	14.9	24
ZIF-8-PBI	-	-	105.4	12.3	25
GO	9.0	1	-	3400	7
GO	4000-6000	0.117	-	30	26
EFDA-GO	1000	4.017	1200	29	27
	100	17.0	507.8	17.4	
CTF-1 membrane	210	11.6	727.6	19.6	This work
	290	8.6	744.9	22.3	

References

[1] P. Kuhn, M. Antonietti, A. Thomas, *Angew. Chem. Int. Ed.*, 2008, **47**, 3450.

[2] M. Rozenberg, A. Loewenschuss, Y. Marcus, *Phys. Chem. Chem. Phys.*, 2000, **2**, 2699.

[3] J. Shen, G. Liu, K. Huang, W. Jin, K.R. Lee, N. Xu, *Angew. Chem. Int. Ed.*, 2015, **54**, 578.

[4] N. I. Kovtyukhova, T. E. Mallouk, L. Pan, E. C. Dickey, J. *Am. Chem. Soc.*, 2003, **125**, 9761.

[5] M. Yoonessi, Y. Shi, D. A. Scheiman, M. Lebron-Colon, D. M. Tigelaar, R. A. Weiss, M. A. Meador, *ACS Nano*, 2012, **6**, 7644.

[6] L. M. Robeson, *J. Membr. Sci.*, 2008, **320**, 390.

[7] H. Li, Z. Song, X. Zhang, Y. Huang, S. Li, Y. Mao, H. J. Ploehn, Y. Bao, M. Yu, *Science*, 2013, **342**, 95.

[8] C. Zhang, Y. Xiao, D. Liu, Q. Yang, C. Zhong, *Chem. Commun.*, 2013, **49**, 600.

[9] N. Wang, A. Mundstock, Y. Liu, A. Huang , J. Caro, *Chem. Eng. Sci.*, 2015, **124**, 27.

[10] Z. Zhao, X. Ma, Z. Li , Y. S. Lin, *J. Membr. Sci.*, 2011, **382**, 82.

[11] M. Sadrzadeh, K. Shahidi , T. Mohammadi, *J. Membr. Sci.*, 2009, **342**, 327.

[12] X. Zhang, Y. Liu, S. Li, L. Kong, H. Liu,Y. Li, W. Han, K. L. Yeung, W. Zhu,W. Yang, J. Qiu, *Chem. Mater.*, 2014, **26**, 1975.

[13] Y. S. Li, F. Liang, H. Bux, A. Feldhoff, W. Yang, J. Caro, *Angew. Chem. Int. Ed.*, 2010, **49**, 548.

[14] F. Zhang, X. Zou, X. Gao, S. Fan, F. Sun, H. Ren, G. Zhu, *Adv. Funct. Mater.*, 2012, **22**, 3583.

[15] S. Zhou, X. Zou, F. Sun, H. Ren, J. Liu, F. Zhang, N. Zhao, G. Zhu, *Int. J. Hydrogen Energy*, 2013, **38**, 5338.

[16] H. Guo, G. Zhu, I. J. Hewitt, S. Qiu, *J. Am. Chem. Soc.*, 2009, **131**, 1646.

[17] A. Huang, Q. Liu, N. Wang, Y. Zhu, J. Caro, *J. Am. Chem. Soc.*, 2014, **136**, 14686.

[18] Y. Hu, J. Wei, Y. Liang, H. Zhang, X. Zhang, W. Shen, H. Wang, *Angew. Chem. Int. Ed.*, 2016, **55**, 2048.

[19] Y. Huang, Y. Xiao, H. Huang, Z. Liu, D. Liu, Q. Yang and C. Zhong, *Chem. Commun.*, 2015, **51**, 17281.

[20] Y. Peng, Y. Li, Y. Ban, H. Jin, W. Jiao, X. Liu, W. Yang, *Science*, 2014, **346**, 1356.

[21] D. Wang, Z. Wang, L. Wang, L. Hu, J. Jin, *Nanoscale*, 2015, **7**, 17649.

[22] M. Yu, H. H. Funke, R. D. Noble, J. L. Falconer, *J. Am. Chem. Soc.*, 2011, **133**, 1748.

[23] S. N. Wijenayake, N. P. Panapitiya, S. H. Versteeg, C. N. Nguyen, S. Goel, K. J. Balkus, J. I. H. Musselman, J. P. Ferraris, *Ind. Eng. Chem. Res.*, 2013, **52**, 6991.

[24] T. Yang, Y. Xiao, T. S. Chung, *Energy Environ. Sci.*, 2011, **4**, 4171.

[25] T. Yang, G. M. Shi, T. S. Chung, *Adv. Energy Mater.*, 2012, **2**, 1358.

[26] H.W. Kim, H. W. Yoon, S.-M. Yoon, B. M. Yoo, B. K. Ahn,Y. H. Cho, H. J. Shin, H. Yang, U. Paik, S. Kwon, J.-Y. Choi, H. B. Park, *Science*, 2013, **342**, 91.

[27] J. Shen, G. Liu, K Huang, Z. Chu, W. Jin, N. Xu, *ACS Nano*, 2016, **10**, 3398.